Published in final edited form as:
J Mol Biol. 2012 March 2; 416(4): 571–578. doi:10.1016/j.jmb.2011.12.055.

The antibiotic thermorubin inhibits protein synthesis by binding to inter-subunit bridge B2a of the ribosome

David Bulkley[1], **Francis Johnson**[2], and **Thomas A. Steitz**[1,3,4,*]

[1]Department of Chemistry, Yale University

[2]Department of Pharmacological Sciences, School of Medicine, Stony Brook University

[3]Department of Molecular Biophysics and Biochemistry, Yale University

[4]Howard Hughes Medical Institute, New Haven, CT 06511

Abstract

Thermorubin is a small molecule inhibitor of bacterial protein synthesis, but relatively little is known about the molecular mechanism by which it blocks translation. The structure of the complex between thermorubin and the 70S ribosome from *Thermus thermophilus* reported here shows that thermorubin interacts with the ribosome in a way that is distinct from any other known class of ribosome inhibitor. Though it is structurally similar to tetracycline, it binds to the ribosome at an entirely different location - the interface between the small and large subunits that is formed by intersubunit bridge B2a. This region of the ribosome is known to play a role in the initiation of translation, and thus the binding site we observe is consistent with evidence suggesting that thermorubin inhibits the initiation stage of protein synthesis. The binding of thermorubin induces a rearrangement of two bases on helix 69 of the 23S rRNA and presumably this rearrangement blocks the binding of an A-site tRNA, thereby inhibiting peptide bond formation. Due in part to its low solubility in aqueous media, thermorubin has not been used clinically, although it is a potent antibacterial agent with low toxicity (Theraputic Index > 200). The interactions between thermorubin and the ribosome, as well as its adjacency to the observed binding sites of three other antibiotic classes, may enable the design of novel derivatives that share thermorubin's mode of action but possess improved pharmacodynamic properties.

Introduction

Small molecule inhibitors of bacterial protein synthesis are widely used as antibiotics [1]. In part because of misuse of these agents, drug-resistant bacteria eventually arise for each antibiotic, necessitating the development of new antibiotics [2]. Unfortunately, drug discovery has not kept pace with the increase in bacterial resistance, and the current need for new antibiotics to treat infectious diseases, especially those of nosocomial origin, is outstripping supply [3]. Thus, identifying new ways to target bacterial protein synthesis may lead to the creation of new antibiotics that are capable of addressing this issue. Here we show that the little-studied antibiotic thermorubin binds to the 70S ribosome from *T.thermophilus* in a way

*To whom correspondence may be addressed. thomas.steitz@yale.edu.

Accession Numbers: atomic coordinates were deposited under PDB accession numbers 3UXQ, 3UXR, 3UXS, 3UXT.

that is distinct from related ribosomal inhibitors but adjacent to the binding sites of different families of antibiotics, thus opening up the possibility of developing new antibiotic compounds.

Thermorubin is a natural product that was isolated from *Thermoactinomyces antibioticus*, a thermophilic actinomycete that grows best at ~50°C [4]. Besides having antibiotic properties, it has been shown also to be a potent aldose reductase inhibitor [5]. Its mechanism of action as an antibiotic is the inhibition of protein synthesis in both Gram-positive and Gram-negative bacteria, but it is inactive against yeast, fungi and higher eukaryotes [6]. Relatively strong activity has been reported against several bacteria, including *Staphylococcus aureus* (MIC = 0.006 μg/mL), *Streptococcus pyogenes* (MIC = 0.025 μg/mL) and *Streptococcus pneumonia* (MIC = 0.05 μg/mL) [7]. Its structure bears a superficial resemblance to that of the tetracyclines (TCs), since its core is a linear tetracycle, but it differs in being a totally aromatic anthracenopyranone, and surprisingly it does not contain a single chiral center. Unlike the TCs, thermorubin binds to both the large and small ribosomal subunits with roughly equal affinity (K_d = 1–2μM), but binds one hundred-fold more tightly to the full 70S particle [8], suggesting a single high affinity binding site on the 70S assembly that is formed by two separate contributions from regions on the large and small subunits.

Thermorubin is also capable of chelating two magnesium ions under intracellular ionic concentrations. Thermorubin is able to inhibit protein synthesis, but only under certain conditions. First, it does not inhibit poly(U)-directed poly(Phe) synthesis at low magnesium concentrations (5mM) or in the absence of initiation factors [6], nor does it affect the reactivity of puromycin with the 70S ribosome complex with AcPhe-tRNA and poly(U) [9]. However, when initiation factors are also present, thermorubin inhibits both poly(U)-directed poly(Phe) synthesis and the binding of fMet-tRNA to the 70S ribosome [6]. Interestingly, it is also able to block poly(U)-directed poly(Phe) synthesis when the magnesium concentration is raised to 12 mM [9]. Finally, thermorubin promotes subunit association at magnesium concentrations that ordinarily promote subunit dissociation [8].

We have determined the crystal structure of thermorubin in complex with the 70S ribosome from *T. thermophilus* and observe that it binds to the ribosome in the vicinity of inter-subunit bridge B2a and near the binding sites of several other ribosomal inhibitors [10; 11; 12]. However, thermorubin binds in a way that is distinct from these other compounds and causes a unique conformational change of the ribosomal RNA. This, combined with the fact that thermorubin apparently targets the initiation stage of protein synthesis, has led us to conclude that the mechanism by which thermorubin inhibits protein synthesis is functionally different from these previously studied compounds.

Results

We determined the co-crystal structure of thermorubin in complex with the 70S ribosome from *T. thermophilus* at 3.2 Å resolution, and the resulting statistics are shown in Table 1. The structure was solved by molecular replacement using a model of the 70S ribosome [13] and refinement was carried out using the PHENIX package[14]. Coordinates for thermorubin were withheld during refinement of the structure, and an unbiased F_o-F_c difference Fourier electron density map was used to position the small molecule crystal structure of thermorubin[15] on the 70S ribosome.

Thermorubin interacts with both the large and small subunits

We observe that thermorubin interacts with both the large and small subunits (Figure 1), which is consistent with available biochemical evidence [8]. The antibiotic binds between helix 69 of the 23S RNA and helix 44 of the 16S RNA in the region of inter-subunit bridge

B2a (Figure 2a). This binding site, which is shared equally between both subunits, explains why thermorubin is able to bind either the large or small subunits individually, as well as the full 70S particle. The tetracylic moiety of thermorubin stacks against the bases of C1409 and G1491 of the small subunit and A1913 of the large subunit (Figure 1). The base of U1915 of the 23S RNA supplies an additional stacking interaction with the drug's orthohydroxyphenyl moiety. Residues C1409 and A1913 also appear to form hydrogen bonds with the antibiotic at oxygens 3 and 4 via their 2'-hydroxyl groups. Finally, our data suggest that two cationic species coordinate the drug, bridging metal chelating sites on the antibiotic and electron-rich regions of the ribosomal RNA. These interactions most likely involve magnesium ions, although the second site is very tightly coordinated, and thus may not be sufficiently large to accommodate a magnesium ion. The presence of two bound cations is consistent with the observation that thermorubin chelates two magnesium ions in solution[8].

Rearrangement of the bases of C1914 and A1913

The binding of thermorubin causes conformational changes of the ribosomal RNA that have important functional consequences. The bases of A1913 and C1914 lie at the tip of helix 69 on the 23S RNA, and when thermorubin binds, the bases of these residues are repositioned (Figure 2b). The adenine at position 1913 moves up towards thermorubin's binding site and stacks against the aromatic tetracycle of the antibiotic. Also, the coordination of the N1 of A1913 with the magnesium ion that is bound by oxygens 6 and 7 of thermorubin further stabilizes this rearrangement. A slight movement of the sugar at position 1913 also takes place, facilitated by the formation of a hydrogen bond between the 2'-OH on the ribose sugar and oxygen 4 of thermorubin. While A1913 moves towards thermorubin, C1914 is pushed away. The base of C1914 ordinarily stacks against the base of U1915 [10; 13; 16], but the terminal orthohydroxy phenyl moiety of the drug displaces the base of C1914 from its stacking interaction and forms a hydrogen bond with the 2' hydroxyl on the ribose sugar of C1409 via oxygen 3. With this position blocked, the base of C1914 rotates out, away from the central axis of helix 69 and into the region normally occupied by a bound A-site tRNA (Figure 3b).

Discussion

Our observation that the conformational change produced by the binding of thermorubin is likely to block the binding of an A-site tRNA is consistent with biochemical evidence suggesting that the binding of thermorubin to the 70S ribosome blocks the initiation phase of bacterial protein synthesis. Thermorubin has relatively little effect on *in vitro* poly(U) dependent poly-phenylalanine synthesis, a process that bypasses the normal route of translation initiation [6; 9], whereas thermorubin effectively inhibits the *in vitro* translation of an endogenous mRNA containing a start codon and Shine-Dalgarno sequence [6]. While poly(U) dependent poly-phenylalanine synthesis is not inhibited by thermorubin under physiological magnesium concentrations (6mM), the drug is able to block poly-phenylalanine synthesis under elevated magnesium concentrations (12mM) [9]. Interestingly, the level of inhibition that can be achieved depends on whether thermorubin is introduced before or after poly(U) is added to the system. Prior incubation of 70S particles with thermorubin leads to near-complete inhibition of polyphenylalanine synthesis, while simultaneous addition of poly(U) and thermorubin leads only to a 30% reduction of poly-phenylalanine synthesis even at the highest concentrations of thermorubin. The structure of the complex between thermorubin and the 70S ribosome suggests that an A-site tRNA and thermorubin could not simultaneously occupy the ribosome (Figure 3b). Thus, it may be that thermorubin preferentially binds during the initiation phase because a ribosome at this stage of protein synthesis is more likely to have an A-site that is vacant of tRNA.

It has also been observed that thermorubin is able to prevent initiator tRNA from binding to the *E.coli* ribosome when initiation factors are present[9]. The region of the ribosome at which thermorubin binds, inter-subunit bridge B2a (Figure 2a), has been shown to play a role in factordependent translation initiation [17; 18] and IF1 and IF2 have been observed to make contacts with this region [19; 20; 21; 22]. Both C1914 and A1913 lie adjacent to IF2 when it is bound in a 70S initiation complex, and both of these bases are repositioned by the binding of thermorubin. Thus, the rearrangement of C1914 and A1913 may alter the interaction between bridge B2a and initiation factors in such a way that the binding of initiator tRNA in the P-site is blocked. From the structure presented here, it is clear that thermorubin alone would have relatively little effect on the accommodation of a P-site tRNA during translation initiation. Instead, our data show that the binding of thermorubin repositions the base of C1914 of the 23S RNA into the A-site, which would clash with an accommodated A-site tRNA, not an initiator tRNA in the P-site. As we do not know exactly which stage of initiation thermorubin inhibits, it is also possible that f-Met tRNA is accommodated in the P-site, but it is the decoding of the first A-site bound tRNA that is inhibited. Bridge B2a is dispensable for *in vitro* protein synthesis, but its removal by deletion or mutation of helix 69 is lethal to *E. coli* cells [23; 24], raising the possibility that thermorubin interferes with another aspect of bridge B2a function by binding to this region of the ribosome.

In addition to its role in translation initiation, bridge B2a links the large and small subunits during inter-subunit ratcheting, which occurs during the elongation phase of protein synthesis [25]. Thermorubin binds in a cleft formed by helix 69 and helix 44 at the edge of bridge B2a and could be expected to increase the stability of this region of the inter-subunit bridge. It has been shown that bridge B2a undergoes at least a 7Å movement during ratcheting [26], and it is possible that thermorubin prevents this motion by rigidifying the link between helix 69 and helix 44. Two observations support this idea. The first is that thermorubin prevents dissociation of the 70S ribosome into subunits [15]. Second, thermorubin inhibits protein synthesis at higher magnesium concentrations (above 12 mM) [9], suggesting that the combined stabilizing effects of high magnesium and thermorubin cooperatively block translation by limiting inter-subunit mobility.

While thermorubin is a potent inhibitor of ribosomes from both Gram-positive and Gramnegative bacteria, it is essentially inactive against ribosomes from yeast, fungi [4], and higher eukaryotes [7]. This specificity is explained by differences in the structures of the eukaryotic and prokaryotic ribosomal RNA that form the thermorubin binding site. Upon binding to the bacterial ribosome, the tetracyclic, aromatic region of thermorubin stacks against the bases of C1409 and G1491, which form a Watson-Crick base pair (Figure 1). In the yeast 80S ribosome, the equivalent bases C1646 and A1754 are not capable of forming a Watson-Crick base pair, suggesting that they may not be able to accommodate thermorubin. Examination of the crystal structure of the yeast 80S ribosome reveals that A1754 base pairs with U1647 (one residue above C1646, the equivalent of *E. coli* base C1409), and thereby eliminates the long, flat, aromatic surface against which thermorubin packs when bound to the prokaryotic ribosome [27]. It would be interesting to see whether mutation of G1491 to an adenosine in *E.coli* would render the bacterial ribosome resistant to thermorubin. Because thermorubin may depend on initiation factors to inhibit protein synthesis, it is possible that its prokaryotic specificity is also a result of differences between how prokaryotic and eukaryotic translation initiation factors interact with the ribosome.

Despite its potency against a variety of gram positive and gram negative bacteria *in vitro*, thermorubin is relatively ineffective in the treatment of bacterial infections when administered orally or intravenously [7]. It is likely that the compound's limited solubility in aqueous solution prevents it from reaching the site of infection, given that thermorubin is effective against *Streprococcus pyogenes* only when administered intraperitoneally [4].

Consequently, chemical modifications of thermorubin will be necessary to improve its pharmacokinetic characteristics to enable the compound to be used clinically. The location of thermorubin next to the binding sites of three other families of antibiotics[10; 11; 12] identifies and further extends a contiguous antibiotic binding surface that can be used for the structurebased design of novel antibacterial substances (Figure 3c). Perhaps a completely *de novo* drug could be designed to target the large ribosomal surface seen to bind these four antibiotics; a similar strategy is being implemented successfully by Rib-X Pharmeceuticals[28] to obtain a new antibiotic class that targets the bacterial peptidyl transferase center[29].

Materials and Methods

Thermorubin was isolated from *Thermoactinomyces antibioticus* as reported previously[4]. 70S ribosomes from *T. thermophilus* were purified and crystalized according to previously published work, with minor adjustments in the crystallization procedure [30]. Briefly, purified 70S ribosomes were diluted to 10 mg/mL in buffer composed of 5 mM Hepes pH 7.5, 50 mM KCl, 10 mM NH_4Cl and 10 mM $MgAc_2$ and then equilibrated via sitting drop vapor diffusion against a reservoir solution made up of 2.9% (w/v) PEG 20K, 9% (v/v) MPD, 175 mM L-arginine and 100 mM Tris-HCl pH 7.6. Immediately prior to equilibration, the ribosome-containing solution was mixed in a ratio of 3 to 4, ribosome to reservoir solution. Crystals appeared after approximately 4 days and were harvested after 8 days. Following stabilization by gradually increasing the concentration of 2-methyl-2,4-pentanediol to 40% (v/v), thermorubin was added to the mother liquor at a concentration of 100 μM. After 12 hours of equilibration, the crystals were flash frozen in a nitrogen cryostream at 80 K. Diffraction data were collected at the National Synchrotron Light Source on beamline X-25 using a Pilatus 6M detector. Data reduction was performed with the program XDS [31] and an initial solution was generated by molecular replacement with PHASER [32] using the *T. thermophilus* 70S ribosome as a search model [13]. The solution was then refined with the PHENIX package [33].

Acknowledgments

This work was supported by NIH grant GM022778 awarded to T.A.S. We would like to thank David Keller for his help with crystal freezing and cryoprotection and the beamlines at BNL (X-29 and X-25) for the use of their facilities and technical assistance with data collection. We thank the Yale Center for Structural Biology staff, particularly Michael Strickler, for assistance with data processing and Gregor Blaha and C. Axel Innis for helpful discussions during manuscript preparation.

Abbreviations

MIC	minimum inhibitory concentration
TCs	tetracyclines

References

1. Wilson DN. The A-Z of bacterial translation inhibitors. Crit Rev Biochem Mol Biol. 2009; 44:393–433. [PubMed: 19929179]
2. Chen LF, Chopra T, Kaye KS. Pathogens resistant to antibacterial agents. Med Clin North Am. 95:647–76. [PubMed: 21679786]
3. Freire-Moran L, Aronsson B, Manz C, Gyssens IC, So AD, Monnet DL, Cars O. Critical shortage of new antibiotics in development against multidrug-resistant bacteria-Time to react is now. Drug Resist Updat. 14:118–124. [PubMed: 21435939]
4. Craveri R, Coronelli C, Pagani H, Sensi P. Thermorubin, a New Antibiotic from a Thermoactinomycete. Clin Med (Northfield Il). 1964; 71:511–21. [PubMed: 15446134]

5. Hayashi K, Dombou M, Sekiya M, Nakajima H, Fujita T, Nakayama M. Thermorubin and 2-hydroxyphenyl acetic acid, aldose reductase inhibitors. J Antibiot (Tokyo). 1995; 48:1345–6. [PubMed: 8557578]
6. Pirali G, Somma S, Lancini GC, Sala F. Inhibition of peptide chain initiation in Escherichia coli by thermorubin. Biochim Biophys Acta. 1974; 366:310–8. [PubMed: 4609482]
7. Cavalleri B, Turconi M, Pallanza R. Synthesis and antibacterial activity of some derivatives of the antibiotic thermorubin. J Antibiot (Tokyo). 1985; 38:1752–60. [PubMed: 4093335]
8. Lin F, Wishnia A. The protein synthesis inhibitor thermorubin. 1. Nature of the thermorubin-ribosome complex. Biochemistry. 1982; 21:477–83. [PubMed: 7039671]
9. Lin F, Wishnia A. The protein synthesis inhibitor thermorubin. 2. Mechanism of inhibition of initiation on Escherichia coli ribosomes. Biochemistry. 1982; 21:484–91. [PubMed: 7039672]
10. Voorhees RM, Weixlbaumer A, Loakes D, Kelley AC, Ramakrishnan V. Insights into substrate stabilization from snapshots of the peptidyl transferase center of the intact 70S ribosome. Nat Struct Mol Biol. 2009; 16:528–33. [PubMed: 19363482]
11. Stanley RE, Blaha G, Grodzicki RL, Strickler MD, Steitz TA. The structures of the antituberculosis antibiotics viomycin and capreomycin bound to the 70S ribosome. Nat Struct Mol Biol. 17:289–93. [PubMed: 20154709]
12. Borovinskaya MA, Shoji S, Fredrick K, Cate JH. Structural basis for hygromycin B inhibition of protein biosynthesis. RNA. 2008; 14:1590–9. [PubMed: 18567815]
13. Selmer M, Dunham CM, Murphy FVt, Weixlbaumer A, Petry S, Kelley AC, Weir JR, Ramakrishnan V. Structure of the 70S ribosome complexed with mRNA and tRNA. Science. 2006; 313:1935–42. [PubMed: 16959973]
14. Adams PD, Afonine PV, Bunkoczi G, Chen VB, Davis IW, Echols N, Headd JJ, Hung LW, Kapral GJ, Grosse-Kunstleve RW, McCoy AJ, Moriarty NW, Oeffner R, Read RJ, Richardson DC, Richardson JS, Terwilliger TC, Zwart PH. PHENIX: a comprehensive Python-based system for macromolecular structure solution. Acta Crystallogr D Biol Crystallogr. 66:213–21. [PubMed: 20124702]
15. Johnson F, Chandra B, Iden CR, Naiksatam P, Kahen R, Okaya Y, Lin S. Thermorubin. 1. Structure Studies. J Am Chem Soc. 1980; 102:5580–5585.
16. Zhang W, Dunkle JA, Cate JH. Structures of the ribosome in intermediate states of ratcheting. Science. 2009; 325:1014–7. [PubMed: 19696352]
17. Kipper K, Hetenyi C, Sild S, Remme J, Liiv A. Ribosomal intersubunit bridge B2a is involved in factor-dependent translation initiation and translational processivity. J Mol Biol. 2009; 385:405–22. [PubMed: 19007789]
18. Hirabayashi N, Sato NS, Suzuki T. Conserved loop sequence of helix 69 in Escherichia coli 23 S rRNA is involved in A-site tRNA binding and translational fidelity. J Biol Chem. 2006; 281:17203–11. [PubMed: 16621804]
19. Marzi S, Knight W, Brandi L, Caserta E, Soboleva N, Hill WE, Gualerzi CO, Lodmell JS. Ribosomal localization of translation initiation factor IF2. RNA. 2003; 9:958–69. [PubMed: 12869707]
20. Allen GS, Zavialov A, Gursky R, Ehrenberg M, Frank J. The cryo-EM structure of a translation initiation complex from Escherichia coli. Cell. 2005; 121:703–12. [PubMed: 15935757]
21. Myasnikov AG, Marzi S, Simonetti A, Giuliodori AM, Gualerzi CO, Yusupova G, Yusupov M, Klaholz BP. Conformational transition of initiation factor 2 from the GTP- to GDP-bound state visualized on the ribosome. Nat Struct Mol Biol. 2005; 12:1145–9. [PubMed: 16284619]
22. Carter AP, Clemons WM Jr, Brodersen DE, Morgan-Warren RJ, Hartsch T, Wimberly BT, Ramakrishnan V. Crystal structure of an initiation factor bound to the 30S ribosomal subunit. Science. 2001; 291:498–501. [PubMed: 11228145]
23. Ali IK, Lancaster L, Feinberg J, Joseph S, Noller HF. Deletion of a conserved, central ribosomal intersubunit RNA bridge. Mol Cell. 2006; 23:865–74. [PubMed: 16973438]
24. Liiv A, Karitkina D, Maivali U, Remme J. Analysis of the function of E. coli 23S rRNA helix-loop 69 by mutagenesis. BMC Mol Biol. 2005; 6:18. [PubMed: 16053518]
25. Frank J, Agrawal RK. A ratchet-like inter-subunit reorganization of the ribosome during translocation. Nature. 2000; 406:318–22. [PubMed: 10917535]

26. Dunkle JA, Wang L, Feldman MB, Pulk A, Chen VB, Kapral GJ, Noeske J, Richardson JS, Blanchard SC, Cate JH. Structures of the bacterial ribosome in classical and hybrid states of tRNA binding. Science. 332:981–4. [PubMed: 21596992]
27. Ben-Shem A, Jenner L, Yusupova G, Yusupov M. Crystal structure of the eukaryotic ribosome. Science. 330:1203–9. [PubMed: 21109664]
28. Franceschi F, Duffy EM. Structure-based drug design meets the ribosome. Biochem Pharmacol. 2006; 71:1016–25. [PubMed: 16443192]
29. Skripkin E, McConnell TS, DeVito J, Lawrence L, Ippolito JA, Duffy EM, Sutcliffe J, Franceschi F. R chi-01, a new family of oxazolidinones that overcome ribosome-based linezolid resistance. Antimicrob Agents Chemother. 2008; 52:3550–7. [PubMed: 18663023]
30. Bulkley D, Innis CA, Blaha G, Steitz TA. Revisiting the structures of several antibiotics bound to the bacterial ribosome. Proc Natl Acad Sci U S A. 107:17158–63. [PubMed: 20876130]
31. Kabsch W. Xds. Acta Crystallogr D Biol Crystallogr. 2010; 66:125–32. [PubMed: 20124692]
32. McCoy AJ, Grosse-Kunstleve RW, Adams PD, Winn MD, Storoni LC, Read RJ. Phaser crystallographic software. J Appl Crystallogr. 2007; 40:658–674. [PubMed: 19461840]
33. Adams PD, Afonine PV, Bunkoczi G, Chen VB, Davis IW, Echols N, Headd JJ, Hung LW, Kapral GJ, Grosse-Kunstleve RW, McCoy AJ, Moriarty NW, Oeffner R, Read RJ, Richardson DC, Richardson JS, Terwilliger TC, Zwart PH. PHENIX: a comprehensive Python-based system for macromolecular structure solution. Acta Crystallogr D Biol Crystallogr. 2010; 66:213–21. [PubMed: 20124702]
34. Kleywegt GJ, Jones TA. Detection, delineation, measurement and display of cavities in macromolecular structures. Acta Crystallogr D Biol Crystallogr. 1994; 50:178–85. [PubMed: 15299456]

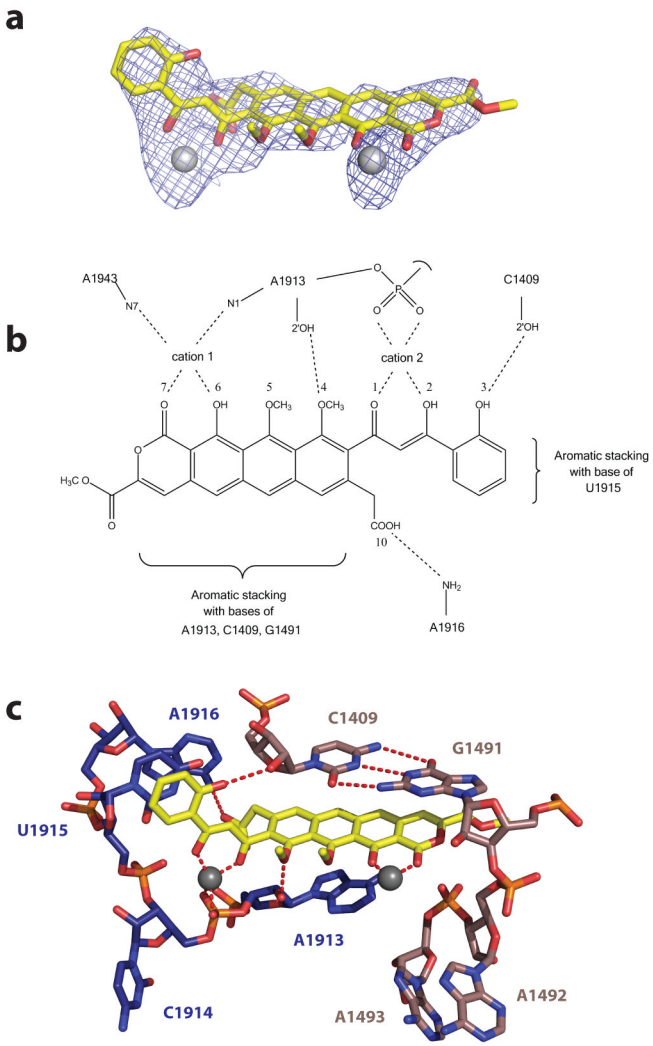

Figure 1.

Interactions between thermorubin and the ribosome. (a) An unbiased F_o-F_c difference Fourier map of thermorubin in complex with the *T. thermophilus* 70S ribosome. The difference electron density is contoured at 3σ, with the corresponding model for thermorubin shown in yellow, oxygen atoms in red, and two putative ions shown as grey spheres. (b) The chemical structure of thermorubin with the positions of various oxygen atoms numbered. The diagram also shows interactions between the drug and cations as well as nucleotides of the ribosomal RNA. (c) Detailed view of the binding site of thermorubin. The antibiotic is shown in yellow, with residues of the 16S RNA shown in beige and residues of the 23S RNA in purple.

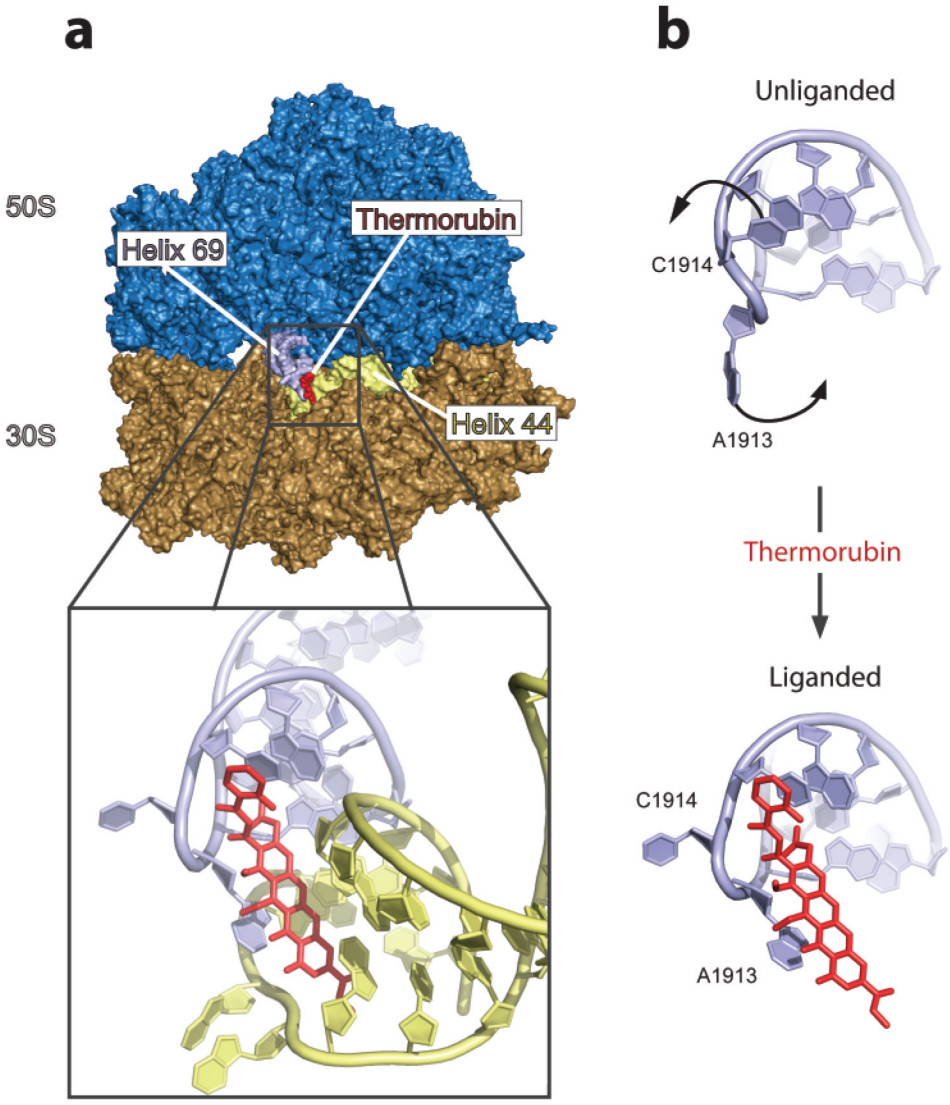

Figure 2.

The binding site of thermorubin. (a) An overview of the ribosome in complex with thermorubin. The large subunit is shown in blue and the small subunit in gold, with thermorubin in red. A close up view of thermorubin bound to the ribosome shows the drug nestled between helix 69 (blue-grey) of the large subunit and helix 44 (yellow) of the small subunit. (b) Conformational changes in residues C1914 and A1913 of helix69 of the large ribosomal subunit induced by the binding of thermorubin. The “unliganded” helix 69 shown above is taken from a structure of the complex between aminoacylated tRNA, paromomycin and the 70S ribosome (PDB code 2WDI)[11]. The “liganded” helix 69 shown below is the complex between thermorubin and the 70S ribosome.

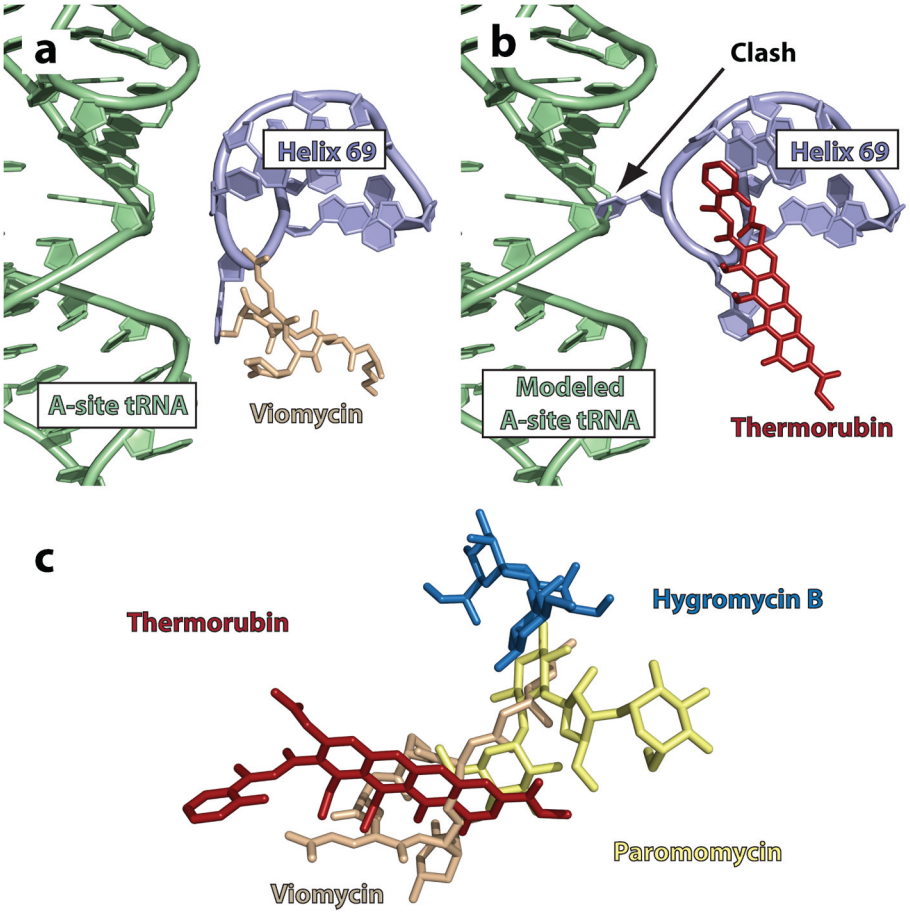

Figure 3.

Comparison between the positions of thermorubin and other antibiotics that bind in the region of intersubunit bridge B2a. (a) Orientation of helix 69 with A-site tRNA and viomycin in complex with the 70S ribosome (PDB codes 3KNH and 3KNI). The antibiotic viomycin is shown in tan, A-site tRNA in green and helix 69 in blue. (b) Orientation of helix 69 when thermorubin is bound. A-site tRNA[11] (PDB 3KNH) is superimposed to show that reorientation of residue C1914 when thermorubin binds would result in a clash between accommodated A-site tRNA and helix 69 of the 23S RNA. (c) Superimposition of thermorubin with viomycin[11] (PDB 3KNH), paromomycin[10] (PDB 2WDG) and hygromycin B[12] (3DF1), other antibiotics that bind in the vicinity of intersubunit bridge B2a. Each structure was superimposed using the phosphate backbone of the 16S RNA in the program LSQMAN[34].

Table 1

Data collection and refinement statistics for 70S·thermorubin complex

Data collection	
Space group	$P2_12_12_1$
Cell dimensions	
a, *b*, *c* (Å)	210.1, 449.4, 621.7
Resolution (Å)	50-3.2 (3.28-3.20)
R_{mrgd} (%)	20.7 (87.0)
I/σI	9.09 (1.92)
Completeness	(%) 99.9 (99.9)
Redundancy	7.6 (7.3)
Refinement	
R_{work} (%)	24.3
R_{free} (%)	27.2
Bond rmsd (Å)	0.010
Angle rmsd (°)	1.14